Onset of Superfluidity in Small $CO_2(^4He)_N$ Clusters

F. Paesani,[1] Y. Kwon,[2] and K. B. Whaley[1]

[1]*Department of Chemistry and Pitzer Center for Theoretical Chemistry, University of California, Berkeley, California 94720, USA*
[2]*Department of Physics, Konkuk University, Seoul 143-701, Korea*

We provide definitive theoretical evidence for the onset of superfluidity in small helium clusters doped with molecules at less than one solvation shell, with quantitative analysis of spectroscopic constants for CO_2 in ^4He_N in terms of nonclassical rotational inertia and helium superfluidity calculated by path integral methods. We find a significant superfluid response for $N \geq 5$, with essentially unit response to rotations around the CO_2 axis and partial response to rotations about an axis perpendicular to the CO_2 axis for $N \geq 6$. This anisotropic superfluid response is shown to be responsible for the N dependence of measured CO_2 rotational spectra in ^4He_N.

Feynman path integrals provide a microscopic analysis of superfluidity in Bose systems that allows the superfluid response to be quantified in terms of exchange-coupled imaginary-time paths of the Bose particles at finite temperatures. Such analysis has revealed that, independent of the number of Bose particles, superfluidity arises when these paths enclose an area comparable to the system size [1] and path integral Monte Carlo calculations have shown that significant superfluid fractions are present in ^4He clusters with a few tens of atoms [2,3] as well as in para-hydrogen clusters small enough to be liquid [4–6]. In the last several years, the spectroscopy of molecules embedded in helium droplets has been shown to offer a unique possibility of studying the superfluid properties of ^4He in finite systems ranging from a few atoms via nanoscale clusters to large droplets [7].

One of the most striking features emerging from these spectroscopic studies is the phenomenon of free rotation of a dopant molecule in large ^4He droplets, which is generally accompanied by some renormalization of its effective rotational constant, B (see, e.g., Table III in Ref. [7]). Evolution of the effective molecular spectroscopic constants with the number N of helium atoms has also become a subject of much interest following an early theoretical analysis made for SF_6 in small ^4He clusters that showed a monotonic decrease of B from the gas phase value as N increases up to ≈ 8, at which size saturation to the large droplet value was seen [8]. Recently, infrared and microwave spectra of molecules have been observed also in small clusters as ^4He atoms are added one by one. Measurements for the carbonyl sulfide (OCS) molecule have revealed the predicted monotonic decrease of B [9] although for this linear molecule the experimental value is seen to undershoot the droplet value, implying a turnaround at larger cluster sizes. Quantum calculations of rotational excitations for $OCS(^4He)_N$ clusters have subsequently demonstrated that this initial decrease of B is indeed followed by a slow increase to values approaching the droplet limit for N less than one solvation shell [10,11].

Recent measurements of the spectra of N_2O [12] and of CO_2 [13] in small ^4He clusters have validated these theoretical predictions, showing an initial decrease of B that is followed by a turnaround (at $N \approx 7$–8 for N_2O and at $N \approx$ 5–6 for CO_2) to saturation to an approximately constant value for larger sizes. In both experimental studies [12,13] the nonuniform decrease of B for N_2O and CO_2 has been explained by invoking the decoupling of a fraction of the helium density from the rotational motion of the molecule predicted in [8,14]. Theoretical and experimental studies have called for investigations to determine whether this behavior is the result of the onset of permutation exchanges among ^4He atoms and therefore a manifestation of incipient superfluid behavior. However, no definitive analysis in terms of superfluid properties has been made to date for the characteristic turnaround of the effective rotational constant for molecules inside helium clusters. This Letter provides such a theoretical analysis for $CO_2(^4He)_N$ clusters, showing that the size dependence of anisotropic superfluid response of helium accounts quantitatively for the evolution of the rotational spectrum of CO_2 in small clusters containing up to one solvation shell of helium.

Within the path integral representation the quantum inertia tensor of an anisotropic Bose liquid can be written in terms of the projected area A_i of the Feynman paths [1]:

$$I_{ij} = I_{ij}^{cl} - \frac{4mk_BT\langle A_iA_j\rangle}{\hbar^2}, \qquad (1)$$

where I_{ij}^{cl} is the classical inertia tensor and the average is taken over the paths of the nonrotating system. Because of the cylindrical symmetry of $CO_2(^4He)_N$, the inertia tensor I_{ij} of the helium component has only two distinguishable principal values, namely, parallel $I_\parallel$ and perpendicular $I_\perp$ components. In linear response, the two effective rotational inertia components of $CO_2(^4He)_N$ are then given by $I_\parallel^{\text{eff}} = I_\parallel$ and $I_\perp^{\text{eff}} = I^{CO_2} + I_\perp$. Since $I_{\parallel(\perp)}$ defines the response of the ^4He density to rotations around an axis coincident with (perpendicular to) the CO_2 axis, $I_\perp^{\text{eff}}$ determines the effec-

tive molecular rotational constant $B = 1/2I_\perp^{eff}$. For CO_2, unlike the other linear molecules OCS [15] and N_2O [16], the helium density distribution is quite insensitive to the molecular rotations, implying that the superfluid density is also insensitive to these. Therefore, the linear response approach is used here, for the first time, to calculate the effective rotational constant of a molecular impurity in ^4He_N clusters as a function of N.

Path integral Monte Carlo calculations are performed here at a temperature $T = 0.15$ K [17]. The low temperature density matrix is factorized as usual into M high temperature density matrices with imaginary-time step $\tau = (Mk_BT)^{-1}$ and the high temperature terms approximated by a product of the free particle propagator and an interaction term [1]. The free particle propagator includes here all translational degrees of freedom but no rotational motions, consistent with Eq. (1). The total interaction potential energy is obtained as a sum of all pairwise contributions. In the present implementation, both isotropic He-He [18] and anisotropic CO_2-He [19] interactions are incorporated using the pair-product form of the exact two-body density matrices that result when the CO_2-He potential energy surface is fitted with a sum of spherical Lennard-Jones interactions [20]:

$$V^{CO_2-He}(R, \vartheta) = \sum_n V_n(|\mathbf{R} - \mathbf{r}_n|) + \Delta V(R, \vartheta). \quad (2)$$

Here, $V_n(|\mathbf{R} - \mathbf{r}_n|)$ is the nth Lennard-Jones potential and $\Delta V(R, \vartheta)$ is the "residual" potential energy surface correction. From symmetry considerations $\mathbf{r}_n \equiv z_n$. The spherical expansion of Eq. (2) allows an exact two-body density matrix to be used for each Lennard-Jones potential, while the residual small contribution $\Delta V(R, \vartheta)$ is treated within the primitive approximation [1]. This approach can greatly reduce the imaginary-time step dependence of all
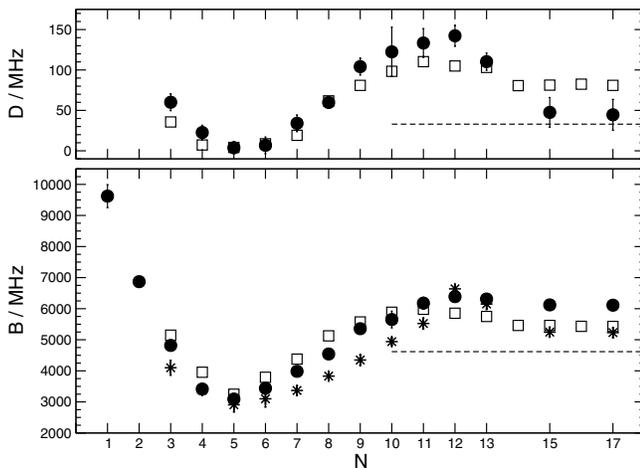
expectation values [21], allowing use of larger τ than otherwise possible. For CO_2, it allows $\tau^{-1} = 40$ K, considerably larger than the typical values required when molecule-He interactions are treated entirely within the primitive approximation [22]. The parameters in Eq. (2) were obtained from minimization of $\Delta V(R, \vartheta)$ using the simulated annealing algorithm. We find that five Lennard-Jones potentials suffice to reproduce the full CO_2-He interaction with great accuracy and minimal $\Delta V(R, \vartheta)$.

Figure 1 shows the linear response estimates $B = 1/2I_\perp^{eff}$ (stars) for $CO_2(^4He)_N$, together with the effective spectroscopic constants (solid circles) obtained by calculating rotational excited states and then fitting these to the linear rotor Hamiltonian

$$E(J) = BJ(J + 1) - DJ^2(J + 1)^2, \quad (3)$$

where B and D are the effective rotational and distortion constants, respectively. The rotational excited states are computed with the projection operator imaginary-time spectral evolution (POITSE) method that has been successfully employed for calculation of the rotational excitations of OCS in ^4He_N [10] and in (para-$H_2)_N$ [23]. Also reported in the figure are the available experimental values (open squares) [13]. All three data sets for the effective rotational constant (bottom panel) show identical nonmonotonic behavior with N. In fact, B first monotonically decreases up to $N = 5$, while a subsequent increase is seen from $N = 6$ to $N \approx 12$, after which B remains approximately constant. The distortion constant D (top panel) also decreases up to $N = 5$, indicating that the structure of the $CO_2(^4He)_5$ cluster is quasirigid, similar to what has been previously found for the analogous $OCS(^4He)_5$. A steep increase in magnitude of D is then found from $N = 6$ to $N = 10$, indicating that very floppy structures are obtained for these sizes. For larger clusters D decreases again, reaching an approximately constant value at $N \geq 15$ [24]. Remarkably good agreement with experimental values is obtained for both B and D constants at all sizes.

The nonmonotonic behavior of the linear response estimate of B as a function of N suggests that the rotational

FIG. 1. Spectroscopic constants B and D for $CO_2(^4He)_N$ clusters. Stars: linear response estimate $B = 1/2I_\perp^{eff}$ obtained from nonclassical rotational inertia; filled circles: POITSE results from Eq. (3); open squares: experimental values [13]; dashed line: experimental droplet value [26].
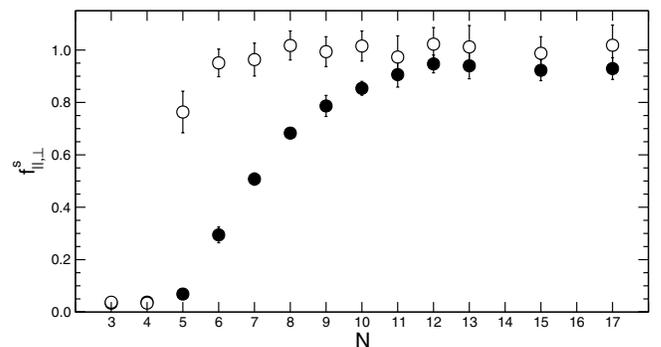
FIG. 2. ^4He superfluid fraction for $CO_2(^4He)_N$ clusters. Open circles: parallel component $f_\parallel^s$; solid circles: perpendicular component $f_\perp^s$.

inertia of the helium solvation density is nonclassical for $N \gtrsim 5\text{-}6$, which implies finite superfluidity. In linear response theory, the global superfluid fraction of a Bose system can be defined by the ratio between the quantum and classical moments of inertia [1]:

$$f^s_{\parallel(\perp)} = 1 - \frac{I_{\parallel(\perp)}}{I^{cl}_{\parallel(\perp)}}. \tag{4}$$

This relation, along with the computed values for the moments of inertia, enables us to estimate both parallel and perpendicular superfluid fractions of the surrounding helium, which are shown in Fig. 2 for the entire size range $N = 3\text{-}17$. [Analysis of the ^{4}He binding energy calculated with diffusion Monte Carlo methods [22] indicates that the first ^{4}He solvation shell around CO_2 is complete at $N \approx 17$.] Both parallel and perpendicular components of f^s are seen to be negligible for $N \leq 4$. The parallel component $f^s_{\parallel}$ then shows a steep increase at $N = 5$, after which it is approximately constant at unit value for all sizes up to $N = 17$. In contrast, the perpendicular component $f^s_{\perp}$ has its first non-negligible value at $N = 6$, after which it shows a monotonic increase up to $N \approx 12$. Beyond $N = 12$, $f^s_{\perp}$ is then also approximately constant, at a value of ~ 0.9. The general agreement in N dependence of the linear response estimate of B with both POITSE and experimental values shown in Fig. 1 provides for the first time clear evidence that the size evolution of perpendicular superfluid fraction $f^s_{\perp}$ is directly responsible for the nonmonotonic behavior observed in the experimentally measured B values.

In order to analyze how local contributions to the helium superfluidity affect the size dependence of molecular rotational properties evident in Fig. 1, we have also computed local superfluid density distributions $\rho^s_{\parallel(\perp)}(\mathbf{R})$ using a local decomposition of Eq. (1) recently proposed by Draeger and Ceperley [20]. Such a local decomposition is not unique, but nevertheless allows qualitative analysis of the relative contributions from different regions in the inhomogeneous solvation layer around the molecule. Density distributions $\rho^s_{\parallel(\perp)}(\mathbf{R})$ are shown for several cluster sizes in Fig. 3, together with the total helium solvation densities. The total density shows formation of an initial equatorial ring around the CO_2 axis for $N \leq 5$ that is located at the global minimum of the molecule-He potential energy surface, as for the analogous $OCS(^4He)_N$ clusters [15]. After this ring is filled by five ^{4}He atoms, the helium density begins to be nonzero also at the two ends of CO_2 and as a result the molecule becomes completely solvated by helium. Figures 2 and 3 show that the first nonzero value of $f^s_{\parallel}$, at $N = 5$, corresponds to an appreciable parallel superfluid density $\rho^s_{\parallel}(\mathbf{R})$ in the global minimum region of the CO_2-He interaction where the helium atoms constitute an annular ring about the molecular axis. In contrast, the perpendicular superfluid density $\rho^s_{\perp}(\mathbf{R})$ is nonzero first at $N = 6$, corresponding to the first non-negligible value of $f^s_{\perp}$, and is already extended along the molecular axis at this
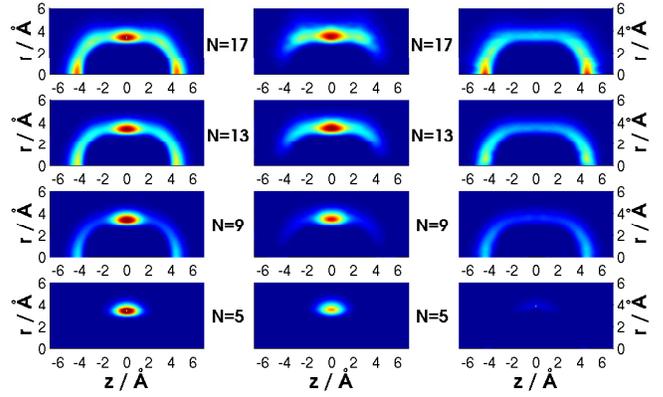
FIG. 3 (color online). ^{4}He density distributions for $CO_2(^4He)_N$ clusters. The CO_2 molecule is located on the z axis with the carbon atom at $z = 0.0$ Å, and the two oxygen atoms at $z = \pm 1.1615$ Å, respectively. Left column: total density $\rho(z, r)$, central column: parallel superfluid density $\rho^s_{\parallel}(z, r)$, right column: perpendicular superfluid density $\rho^s_{\perp}(z, r)$. All densities in Å^{-3}. Color scale goes from 0.0 Å^{-3} (blue; black background outside the grey) to 0.1 Å^{-3} (red; darkest regions inside the grey).

size. Analysis of the length of permutation exchanges shows that the unit value of $f^s_{\parallel}$ for $N = 5$ is essentially due to cyclic permutation exchanges of all five helium atoms located in this ring. These permutations occur in the imaginary-time dynamics and do not result in any angular momentum along the molecular axis. They do not correspond to real rotations of the ring around the CO_2 axis, which require significantly higher energy since the first symmetry-allowed rotation around the CO_2 axis must have $J = 5$ and $K = 5$ [25], where J and K are the total angular momentum and its projection on the CO_2 axis, respectively. For larger cluster sizes, $\rho^s_{\parallel}(\mathbf{R})$ is clearly still primarily localized in the equatorial ring, but now extends increasingly towards the two ends of the CO_2 molecule, while the intensity of $\rho^s_{\perp}(\mathbf{R})$ increases uniformly along the entire molecular axis. This implies the appearance of an increasing number of long permutation exchanges involving ^{4}He atoms located in different regions around the molecule.

Comparison of Fig. 1 with Figs. 2 and 3 now shows how the characteristic N dependence of B results from the onset of anisotropic helium superfluidity. First, we note that a large value of the parallel superfluid component $f^s_{\parallel}$ means negligible response of the helium density to rotations around the CO_2 axis, and hence implies that a negligible component of the total angular momentum is projected on the CO_2 axis. This results in the absence of any Q branch (deriving from rovibrational transitions with selection rules $\Delta J = 0$, $\Delta K = 0$, and $K \neq 0$) in the spectrum and consequent appearance of a linear rotor spectrum for the molecule-helium cluster. Figure 2 thus implies that all but the very smallest clusters, $N \leq 4$ will show linear rotor spectra, which is confirmed by the recent experimental measurements of Tang *et al.* [13]. Next, we see that the

decrease of B apparent in Fig. 1 for the smallest sizes up to $N = 5$ coincides with a negligible value of $f_\perp^s$ in Fig. 2, while an increase for both B and $f_\perp^s$ is seen to start at $N = 6$. For the largest sizes there is also a close correspondence between B and $f_\perp^s$, with both quantities reaching a maximum at $N = 12$ after which they are approximately constant. The less than unit value of $f_\perp^s$ here implies existence of a nonsuperfluid fraction $f_\perp^n = 1 - f_\perp^s$ that is consistent with predictions of a local nonsuperfluid density component in the first solvation shell of larger impurity-doped helium clusters [3,14,20]. In fact, since $I_\perp = I_\perp^{cl}(1 - f_\perp^s) = I_\perp^{cl} f_\perp^n$, the linear response value of B implies that the molecular rotation is rigidly coupled to a nonsuperfluid density component that is characterized on average by the complementary nonsuperfluid fraction $f_\perp^n$ in this first solvation shell. This is strongly supported by the excellent agreement of the linear response values with experiment for $N > 12$. (Increased packing of the first helium solvation shell in larger droplets may account for the somewhat smaller asymptotic B value.)

Further insights are gained from examination of the local superfluid and total ^{4}He density distributions in Fig. 3. With rigid attachment of helium as CO_2 rotates, the density close to the molecular axis and, therefore, located in regions far away from the rotation axis should be more effective in reducing the rotational constant B below its gas phase value. For $N \geq 6$, the increasing helium density located here is predominantly superfluid to rotation around an axis perpendicular to the CO_2 axis and therefore results in a large decrease in the nonclassical rotational inertia $I_\perp$. In contrast, complete rigid coupling to the molecular rotation is the situation for $N \leq 5$, for which $\rho_\perp^s(\mathbf{R})$ is essentially zero. The appearance of significant perpendicular superfluid density at the two ends of the molecule thus constitutes the reason why B turns around at $N = 6$. Conversely, when coming from the large N droplet limit, the turnaround is now seen to correspond directly to the point at which the molecular-interaction induced local nonsuperfluid helium density that constitutes only part of the solvation density in a large cluster [3] becomes equivalent in a small cluster to the total solvation density.

In summary, the present results provide the first direct and quantitative evidence that the onset of superfluidity in doped helium clusters is responsible for the nonmonotonic behavior of effective rotational constants seen at small N, causing a turnaround in B when the rotational inertia becomes nonclassical due to helium superfluidity. Already at less than one solvation layer, the helium constitutes a nanoscale superfluid characterized by a highly anisotropic response to rotation. For rotation around axes perpendicular to the molecular axis the superfluid response saturates at a partial, less than unit value which determines the saturation value of the effective molecular rotation constant, while the parallel superfluid response is essentially unity for $N \geq 5$.

[1] D. M. Ceperley, Rev. Mod. Phys. **67**, 279 (1995).

[2] P. Sindzingre, M. L. Klein, and D. M. Ceperley, Phys. Rev. Lett. **63**, 1601 (1989).

[3] Y. Kwon, P. Huang, M. V. Patel, D. Blume, and K. B. Whaley, J. Chem. Phys. **113**, 6469 (2000).

[4] P. Sindzingre, D. M. Ceperley, and M. L. Klein, Phys. Rev. Lett. **67**, 1871 (1991).

[5] M. C. Gordillo, Phys. Rev. B **60**, 6790 (1999).

[6] Y. Kwon and K. B. Whaley, Phys. Rev. Lett. **89**, 273401 (2002).

[7] For a recent review see, e.g., J. P. Toennies and A. F. Vilesov, Angew. Chem., Int. Ed. **43**, 2622 (2004).

[8] E. Lee, D. Farrelly, and K. B. Whaley, Phys. Rev. Lett. **83**, 3812 (1999).

[9] J. Tang, Y. Xu, A. R. W. McKellar, and W. Jager, Science **297**, 2030 (2002).

[10] F. Paesani, A. Viel, F. A. Gianturco, and K. B. Whaley, Phys. Rev. Lett. **90**, 073401 (2003).

[11] S. Moroni, A. Sarsa, S. Fantoni, K. E. Schmidt, and S. Baroni, Phys. Rev. Lett. **90**, 143401 (2003).

[12] Y. Xu, W. Jager, J. Tang, and A. R. W. McKellar, Phys. Rev. Lett. **91**, 163401 (2003).

[13] J. Tang, A. R. W. McKellar, F. Mezzacapo, and S. Moroni, Phys. Rev. Lett. **92**, 145503 (2004).

[14] Y. Kwon and K. B. Whaley, Phys. Rev. Lett. **83**, 4108 (1999).

[15] F. Paesani and K. B. Whaley, J. Chem. Phys. **121**, 4180 (2004).

[16] F. Paesani and K. B. Whaley, J. Chem. Phys. **121**, 5293 (2004).

[17] Measured temperatures for the $CO_2(^4He)_N$ clusters in Ref. [13] vary between $T \sim 0.15$ and $T \sim 0.7$ K, depending on cluster source conditions (A. R. W. McKellar, private communication).

[18] R. A. Aziz, F. R. W. McCourt, and C. C. K. Wong, Mol. Phys. **61**, 1487 (1987).

[19] G. Yan, M. Yang, and D. Xie, J. Chem. Phys. **109**, 10284 (1998).

[20] E. W. Draeger and D. M. Ceperley, Phys. Rev. Lett. **90**, 065301 (2003).

[21] R. Zillich, F. Paesani, Y. Kwon, and K. Whaley, (to be published).

[22] P. Huang, Y. Kwon, and K. B. Whaley, in *Quantum Fluids in Confinement*, edited by E. Krotscheck and J. Navarro (World Scientific, Singapore, 2002), vol. 4.

[23] F. Paesani, R. E. Zillich, and K. B. Whaley, J. Chem. Phys. **119**, 11682 (2003).

[24] Similar results were obtained in Ref. [13] by using a very similar scheme to POITSE, but employing a slightly different CO_2-He potential energy surface.

[25] G. Herzberg, *Infrared and Raman Spectra of Polyatomic Molecules* (Van Nostrand, Princeton, 1945), p. 400.

[26] K. Nauta and R. E. Miller, J. Chem. Phys. **115**, 10254 (2001).